

# Classification Of Wheat Crop Using Remotely Sensed Multi-Spectral Planet-Scope Temporal Data

Awab Ur Rashid Durrani, Arbab Masood Ahmad

**Abstract:** Agriculture plays a vital role in the economies of developing countries and provide the mainsource of food, income and employment for general public. Monitoring and assessment of the crop yields a crucial task and is critical in ensuring good agricultural management. We propose the monitoring and classification of wheat crops through remote sensing by utilizing satellite imagery. In our research work, we have utilized multi-spectral imagery of Planet-Scope satellite for the classification of wheat crop. The imagery used is a temporal stack of remotely sensed imageries obtained on various dates with reference to the phenological cycle of wheat. We employ three different machine learning classifiers i.e., Artificial Neural Network (ANN), Support Vector Machine (SVM) and Minimum Distance (MD) classifier for the wheat crop classification. Confusion matrix and Kappa Coefficient (Kappa Coefficient) analyzes the performance of these three classifiers. The results obtained shows that ANN with an overall accuracy of 98:7031% and Kappa Coefficient equivalent to 0:9825 outperforms the SVM and MD classifiers having the overall accuracy of 85:2005% and 73:1604% and Kappa Coefficient values of 0:8097 and 0:6455, respectively.

**Index Terms:** Remote sensing, Classification, Temporal, Artificial neural network, Support vector machine, Minimum distance, Planetscope.

## 1 INTRODUCTION

Wheat and associated products are a major source of nutrition in South Asian countries including Pakistan, India, Afghanistan and Bangladesh [1]. Pakistan is a developing country with limited resources for regular monitoring and estimation of wheat crop on a diverse landscape [2]. The lack of proper management of wheat crop and yield statistics results in various issues such as overstocking by stakeholders, over pricing and illegal sales and exports. The existing wheat crops estimation in Pakistan relies on farmers feedback about the harvested crop data, which is greatly susceptible to human manipulation and is therefore not very reliable [3]. Precision agriculture's goal is to increase the intelligence in the production of the agricultural crop, using real-time sensing, control and optimization for enhancing soil-crop health as well as advanced cyber-enabled tools for automated and efficient agricultural crop detection and estimation. The last few decades have witnessed enormous scientific and technological advancement in the field of precision agriculture. One of the marvels of technological advancements is the use of remotely sensed satellite data for monitoring the agricultural crops. Remote sensing has been the center of research and development in the last few decades. The advancement in remote sensing has resulted in an improved satellite imaging systems and highly precised agriculture research [4]. The data obtained through the satellite imagery is vital for usage in agricultural research, geological research and strategic land-use analysis and planning. Remote sensing techniques are used to detect and estimate different types of vegetation [5]. The emerging trends in the field of precision agriculture, advancement in intelligent crop monitoring systems, availability of efficient remote sensing capabilities and accessibility to advanced cyber-physical tools can greatly benefit the agricultural crop monitoring and production. In the past the research has paid less attention to the use of remote sensing technology for crop monitoring, analysis and estimation. This is mainly because of the huge cost incurred due to high resolution satellite imageries, the non availability of accurate data and trained human resources. Lately, the launch of high resolution commercial as well open source satellites have throttled the remote sensing research [6], [7]. Satellite imageries are associated with three main

features namely spatial, spectral and temporal resolutions. Spatial resolution captures per pixel covered area of the land, while the spectral resolution is related to the employed spectral wavelengths from the imaging source. However, temporal resolution pertains to the rotational distance between any two images apart in time but belonging to identical location. The effective utilization of these features help us in the identification and estimation of various types of crops. This manuscript proposes a machine learning based technique for the detection and estimation of wheat crops in the sub-region of Khyber Pakhtunkhwa province of Pakistan. We performed our testing in agricultural research farm of University of Peshawar (UOP) as a pilot region. We utilized temporal based features of wheat crop detection and estimation. The supervised classifiers used for detection and estimation are Artificial Neural Network (ANN), Support Vector Machines (SVM) and Minimum Distance (MD). The rest of the manuscript is organized as follows. Section II discusses the related work. Section III illustrates the study area. Section IV encompasses the data description. The methodology is captured in section V. Section IV demonstrates the results, while Section V concludes the paper.

## 2 RELATED WORK

Crop yield estimation in Pakistan is mainly based on the conducted manual land surveys. The area covered by a crop is estimated by the land record officer known as Patwari, who maintains the land record document known as Girdwari in Pakistan. The data from these surveys are collected by the Agriculture, Irrigation and Planning and Development departments for establishment of policy and decision making purpose. Whereas the final yield estimation is done by the use of sampling techniques, which are approved by provincial agriculture statistics coordination board [8]. The productivity of a crop is dependent on various factors such as soil type, seed variety, fertilizer type and proper timings for sowing these seeds. Therefore, quality and quantity of yield expected from the crop depends on the conditions faced by the crop. Haowei Mu et al make use of multi-temporal MODIS images in order to estimate the crop yield for winter wheat. Histogram dimensionality reduction and time series fusion is

used as an input layer for Convolutional Neural Networks (CNN). CNN network was used to extract the features of winter wheat growth [9]. Omer Vanli et al. compared different classification techniques such as Maximum Likelihood, Support Vector Machine, Condition-based and Nearest Neighbour using Landsat 8 data to estimate wheat crop production. The performance analysis were performed, which showed that the Support Vector Machine classifier performed

**TABLE 1**

BAND COMPOSITION OF PLANETSCOPE'S DOVE

Bands	Names	Wave length (µm)	Resolution (m)
Band-1	Blue	0.49 m	3-5m
Band-2	Green	0.55 m	3-5m
Band-3	Red	0.63 m	3-5m
Band-4	Near Infra-Red (NIR)	0.82 m	3-5m

better than all other employed classifiers [10]. Feng Xu et al. combined Landsat 8 and Sentinel-2 temporal images and performed classification with Random forest classifier, obtaining 93.4% of overall accuracy and compared the obtained results with the classification performance of mono-temporal imagery, which resulted in 76.4% of overall accuracy [11]. Research on the relationship between wheat protein content and wheat agronomic parameters at different growing stages with Landsat TM multi-temporal images has been done by Li Cun-jun et al. using partial least squares [12]. Peng YANG et al. estimated wheat yield using multi-temporal Landsat TM images and GIS based model to improve the yield estimation accuracy of crop growth model [13]. Multiple images of Landsat 5 acquired at different growth stages of wheat crop and its Leaf Area Index (LAI) were calculated for all three stages, i.e. jointing, flowering and milking, for estimating crop growth by S Xiaoyu et al. [14]. Jinran Liu et al. used spectral indices for wheat coverage prediction by using multispectral images collected through Unmanned Aerial Vehicle (UAV) equipped with RedEdge-M sensors [15]. Mengmeng Du et al. listed applications of remote sensing using UAV in agriculture, that have proved to be an effective and efficient way of obtaining field information. Furthermore, the feasibility of utilizing multi-temporal color images acquired from a low altitude UAV-camera system to monitor real-time wheat growth status and to map within-field spatial variations of wheat yield for smallholder wheat growers, was investigated [16]. Wen Zhuo et al. Estimated crop production at a geographical scale over a long period by the soil via images retrieved by a water cloud model that uses SAR and optical data [17]. Liu Liangyun et al. acquired Landsat TM images at different stages of wheat crop for its growth monitoring and yield estimation. Firstly, satellite imagery is utilized at seed time along with its NDVI and then in the second stage the yield estimation model was implemented and tested using three imageries of all three stages i.e. Heading, grain filling and milking of wheat crop [18]. There is an emerging trend in the development of remote sensing based cyber physical system for monitoring of earth resources. In [19], a smart cyber physical system is developed for wastewater management. Remote sensing technologies were utilized to gather large quantity of water quality information and to efficiently process it through cyber interfaces for provision of early information for wastewater treatment and decision making. Similarly, in [20], a space based cyber-physical system is proposed in order to address the rising demand for development of low cost and time efficient satellite system for earth resources monitoring. Furthermore, an adaptive Sensor-Drone-Satellite (SeDS)

system for precision agriculture to overcome the challenges of lower cost and time efficiency is proposed in [21].

### 3 STUDY AREA

In our experimental setup, we considered the research farm of Agriculture University, Peshawar, Pakistan as a pilot region. The selected pilot region which is shown in Fig. 1 consists of various agricultural crops, including wheat, Clover, Mustard and Urban.

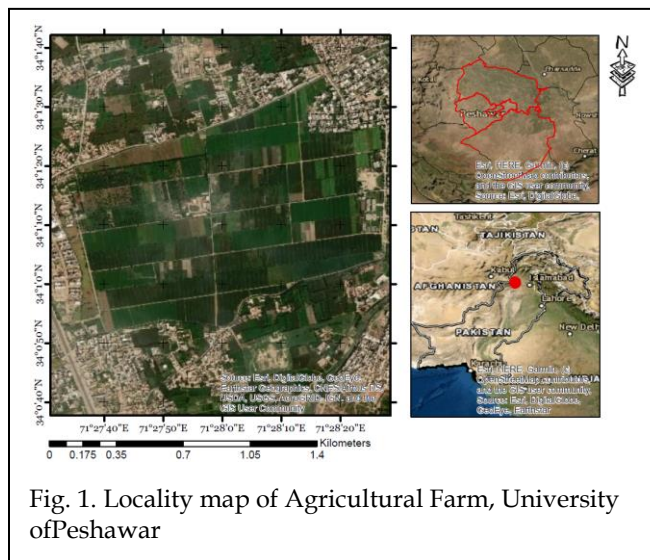


Fig. 1. Locality map of Agricultural Farm, University of Peshawar

### 4 DATA DESCRIPTION

Data used in our research is acquired from Planet Inc. Planet Inc is a private earth imaging company based in California, America. In 2015, the International Space Station (ISS) launched the first Dove nano satellite from on behalf of Planet Inc. Dove has spatial resolution of 2.7m to 3.2m in ISS orbit, while 3.7m to- 4.9m in sun synchronous orbit as presented in Table 1. Dove provides global coverage of 4 channels, including Red, Green, Blue and Near Infrared Reflectance (NIR) to the Geo analysts with a temporal resolution of one day. This makes Dove an attractive option for the observation of Geo events, change detection and monitoring. In this study, the acquired image scenes were atmospherically and radiometrically corrected and the regions of interest used as ground truth data were recorded from all the retrieved scenes.

### 5 METHODOLOGY

Figure 3 represents the process diagram of our adopted methodology. Eight (8) scenes of PlanetScope surface reflectance images were retrieved comprising of 08th and 15th of February, 2nd, 15th and 29th of March and 2nd, 21<sup>st</sup> and 30th of April, 2020. These specific dates for retrieval of PlanetScope imagery were selected while keeping in view the phenological cycle of wheat in Pakistan and favourable climatic conditions. Figure 4 represents time variant spectral characteristics for the selected 8 categories of crops in near infrared (NIR) band. It can be observed from the spectral reflectance curves that wheat crop has highest NIR reflectance profile on 2nd of March. This trend keeps gradually declining till 30th April, when the wheat crop reaches its final stage of growth cycle. A survey for collection of the ground truth data was conducted in the designated pilot region. We

used our native android based Geo survey application i.e., GeoSurvey [22] for conducting the survey. The ground truth data is split into 60% training and 40% test data. The 60% training data is fed to the classifiers for training purpose. In order to validate and evaluate the performance of the considered classifiers, the 40% test set data is used.

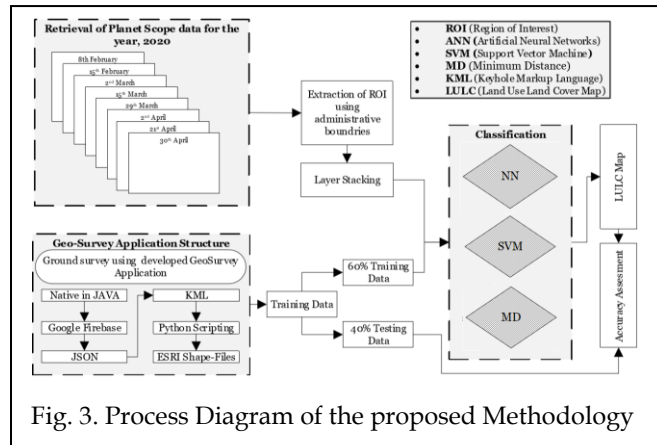


Fig. 3. Process Diagram of the proposed Methodology

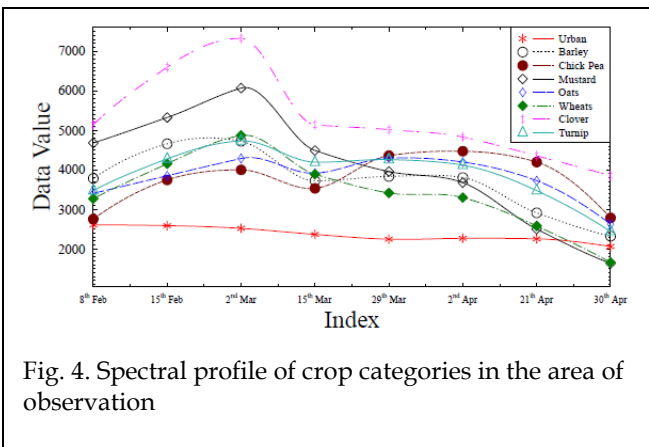


Fig. 4. Spectral profile of crop categories in the area of observation

**5.1 Survey For Ground Truth Data**

A survey to collect the training data was conducted in the designated pilot region using GeoSurvey application. The interface details of the application is provided in Figure 2.

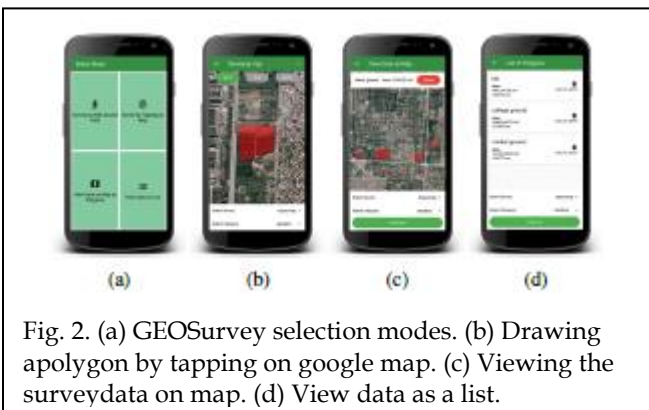


Fig. 2. (a) GEOSurvey selection modes. (b) Drawing a polygon by tapping on google map. (c) Viewing the survey data on map. (d) View data as a list.

- Our survey classes include:
- 1) wheat
  - 2) Urban
  - 3) Turnip

- 4) Clover
- 5) Oats
- 6) Mustard
- 7) Chick Pea
- 8) Barley

The data collected during the survey is saved in Google application development software - firebase. Then it is downloaded in JavaScript Object Notation (JSON) lightweight format, which is converted into Keyhole Mapping Language (KML) file format through python scripting. Such file format can be used to display geographic data in an Earth browser such as Google Earth. ArcGIS is used to convert KML files to shape files into a geospatial vector data format that can be used as training data. The GeoSurvey application for survey has an additional advantage of cost and time effectiveness. The GeoSurvey application can be utilized to perform survey using any of the following two modes:

- Walking survey mode: It can be used by the surveyors for collecting several points from the underlying land cover by walking around the region of interest. Polygon will be drawn on the map once the survey of the field is completed by the surveyor.
- Manual survey mode: It can be used by the surveyors for collecting several points by tapping on the map. Polygon will be drawn on the map once the surveyor completes the points selection on the map for the region of interest.
- Similarly, surveyed data can be viewed using two modes.
- View data as polygon shows polygons of different categories on the google map. Furthermore, view data as a list that captures the list of all polygons
- Each polygon can be associated with a specific category i.e., wheat, Urban, Clover etc.

**5.2 Training**

The training data collected through ground truth surveys is classified into eight different classes. These classes include wheat, Urban, Turnip, Clover, Oats, Mustard, Chick Pea and Barley. The data is divided into 60% training and 40% testing. The training data is fed to classifiers for their training. The performance of the target classifiers is validated against 40% testing data.

**5.3 Accuracy Assessment**

To measure the performance of the proposed mechanism, various accuracy metrics such as overall accuracy, user accuracy, producer accuracy and confusion matrix are considered. These accuracy metrics are explained below.

**5.3.1 Overall Accuracy (OA)**

Overall accuracy is measured by the ratio of exactly classified pixels to the total number of pixels. Mathematically, an overall accuracy is written as:

$$OA = \frac{\text{No. of Exactly classified Pixels}}{\text{Total No. of Pixels}} \quad (1)$$

**5.3.2 User Accuracy (UA)**

The relationship of the exactly classified pixels for a specific class to the total number of pixels classified into that class. It is

related to the error of commission.

$$UA = \frac{\text{Exactlyclassifiedpixelsforaparticularchlass}}{\text{Total\#ofPixelsclassifiedintothatclass}} \quad (2)$$

**5.3.3 Producer Accuracy (PA)**

Producer accuracy is the relationship between exactly classified pixels for a class to the total number of pixels for that class. It is related to the error of omission.

$$PA = \frac{\text{ExactlyClassifiedpixelsforaclass}}{\text{TotalNo.ofPixelsforthatclass}} \quad (3)$$

**5.3.4 Error of Omission (OE)**

Error of omission shows the selection of values that belong to a class but were predicted to be in a different class. They are a measure of false negatives. Errors of omission are shown within columns of the confusion matrix apart from the values along the diagonal. This type of error is additionally referred to as type I error.

$$OE = \frac{\text{ExactlyClassifiedpixelsforaclass}}{\text{TotalNo.ofGroundtruthsamples}} \quad (4)$$

**5.3.5 Error of Commission (OE)**

Errors of commission show the selection of values that were predicted to be in a very class but do not belong to that class. They are a measure of false positives. Errors of commission are shown within rows of the confusion matrix apart from the values along the diagonal. This type of error is referred to as

TABLE 2  
ANN PARAMETERS

Parameters	Values
Training Threshold Contribution	0.9
Training Rate	0.1
Training Momentum	0.9
Training Root Mean Square(RMS) Exit Criteria	0.1
Number of Hidden Layers	1
Number of Training Iterations	500
Min Output Activation Threshold	0.07

type II error.

$$CE = \frac{\text{Incorrectlyclassifiedsites}}{\text{TotalNo.ofclassifiedsites}} \quad (5)$$

**5.4 Supervised Classification Algorithms**

In our experimental setup the following classifiers were employed in order to investigate their classification performance.

**5.4.1 Artificial Neural Networks**

input layer, an output layer, and a hidden layer was used. A multi-layered feed-forward ANN is used to perform nonlinear

classification and uses back propagation for supervised learning. This model has been designed through its motivation from the brain neural system, thus using neural networks in the process. Performance of an ANN classifier can be improved by adjusting weights of the interconnected nodes. The network gives feedback after processing the input data and if there is an error, it is corrected by adjusting the network weights using recursive method [23]. The input values are summed up and passed through activation function. The ANN with temporal features is illustrated visually in Figure 5.

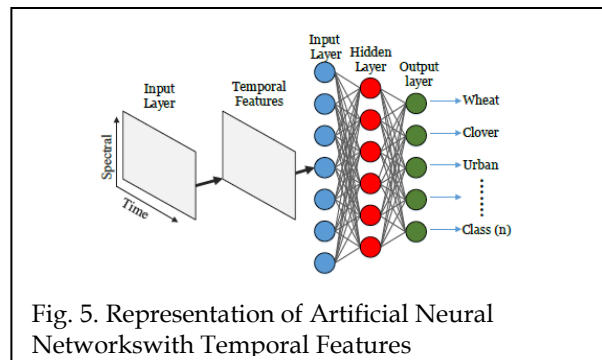


Fig. 5. Representation of Artificial Neural Networks with Temporal Features

Different parameters that control the performance of Neural network are defined as follows;

- Training Threshold Contribution: It helps in determining how much internal weight has contributed with respect to the activation level of the node.
- Training Rate: It works in identifying the magnitude of the weight adjustment for the specific nodes.
- Training Momentum: It helps in preventing the system from converging to a local minimum.
- Training Root Mean Square (RMS) Exit Criteria: RMS error is introduced to stop the algorithm from further training.
- Number of Hidden Layers: It adds additional mathematical calculations.
- Number of Training Iterations: It determines the number of iterations for which training of the algorithm should continue.
- Min Output Activation Threshold: It determines the threshold value for a pixel, below which the pixel is labeled as unclassified.

The values used for various parameters of ANN are shown in Table 2

**5.4.2 Support Vector Machine Classifier (SVM)**

SVM is a supervised, non-parametric classification algorithm derived from statistical learning theory [24]. It separates the considered classes with a decision surface that maximizes the distance between the classes. The decision surface is called a hyper-plane and the decision points that are nearer to hyper-planes are called support vectors which is pictorially presented in Figure 6.

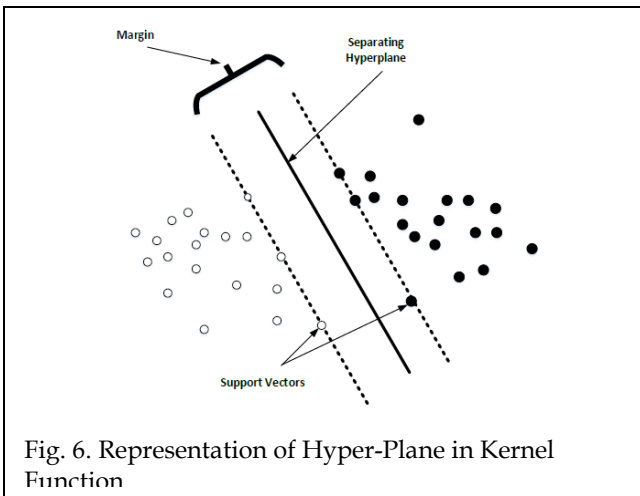


Fig. 6. Representation of Hyper-Plane in Kernel Function

SVM can perform nonlinear classification by using various types of kernels, which converts the nonlinear boundaries to linear one [25]. The SVM classifier is mathematically defined as;

$$w \cdot x + b = 0 \tag{6}$$

Where  $b$  and  $w$  are the parameter of the hyperplane. Vectors which are not in hyper plane are presented by;

$$w \cdot x + b > 0 \tag{7}$$

Whereas the two margins are presented by;

$$w \cdot x + b = -1 \tag{8}$$

And

$$w \cdot x + b = +1 \tag{9}$$

Kernel type: SVM uses various mathematical functions called kernels. Kernel functions take data as input and transform it into the required form. These functions are Linear, Non linear, polynomial, radial basis function (RBF) and sigmoid.

- **Gamma in kernel Function:** Gamma parameter is the inverse of the standard deviation of the RBF kernel. The gamma parameter defines the effect of a single training example, with low values making a loose fit of the training data, while high values make it fit accurately for the model.
- **Penalty parameter:** The penalty parameter 'C' controls the tradeoff between allowing training error and forcing rigid margins. When the value of C is large, the optimization will be a smaller margin hyperplane than training data will be classified correctly.
- **Pyramid Level and Classification Probability Threshold:** Pyramid level sets the number of hierarchical processing levels to apply during the svm training and classification. Where classification probability threshold sets the probability that is required for the svm classifier to classify a pixel. Table 3 present the parameters

TABLE 4  
CLASSIFICATION RESULTS OF ARTIFICIAL NEURAL NETWORKS

Classes	Commission Error %	Omission Error %	Producer Accuracy %	User Accuracy %
Wheat	1.05	0.47	99.53	98.95
Urban	0.00	0.00	100.00	100.00
Turnip	0.67	0.60	99.40	99.33
Clover	0.05	0.04	99.96	99.95
Oats	0.22	0.78	99.22	99.78
Mustard	0.21	0.34	99.66	99.79
Chick Pea	14.71	0.00	100.00	85.29
Barley	0.53	31.95	68.05	99.47
OA	98.7031%			
Kappa Coefficient	0.9825			

TABLE 5  
CLASSIFICATION RESULTS OF SUPPORT VECTOR MACHINES

Classes	Commission Error %	Omission Error %	Producer Accuracy %	User Accuracy %
Wheat	0.44	9.70	90.30	99.56
Urban	0.00	11.93	88.07	100.00
Turnip	0.71	42.66	57.34	99.29
Clover	0.05	3.04	96.96	99.95
Oats	0.52	26.99	73.01	99.48
Mustard	0.15	10.44	89.56	99.85
Chick Pea	0.00	36.62	63.38	100.00
Barley	0.00	54.45	45.55	100.00
OA	85.2005%			
Kappa Coefficient	0.8097			

TABLE 6  
CLASSIFICATION RESULTS OF MINIMUM DISTANCE

Classes	Commission Error %	Omission Error %	Producer Accuracy %	User Accuracy %
Wheat	10.99	30.42	69.58	89.01
Urban	0.00	0.00	100.00	100.00
Turnip	82.87	85.58	14.42	17.13
Clover	4.28	3.65	96.35	95.72
Oats	17.53	55.67	44.33	82.47
Mustard	50.29	18.54	81.46	49.71
Chick Pea	92.88	8.62	91.38	7.12
Barley	68.47	68.41	31.59	31.53
OA	73.1604%			
Kappa Coefficient	0.6455			

values of SVM.

### 5.4.3 Minimum Distance Classifier (MD)

The Minimum distance (MD) is a supervised learning algorithm and is used to classify unknown image data to classes of known labels by minimizing the distance between the imagedata and the class in multi-feature space [26]. The distance measured between the labeled class and unknown imagedata is normally the euclidean distance and is defined as an index of similarity [27]. Typically, the minimum distance is identical to maximum similarity. The mean vector of each class is used to calculate the euclidean distance from the class to the unknown pixel. A pixel of the unknown label is classified to the nearest class unless a distance threshold is specified as shown in Figure 7. In case a pixel does not meet the defined criteria, it is labeled as unclassified [28]. The euclidean distance is defined mathematically as follow;

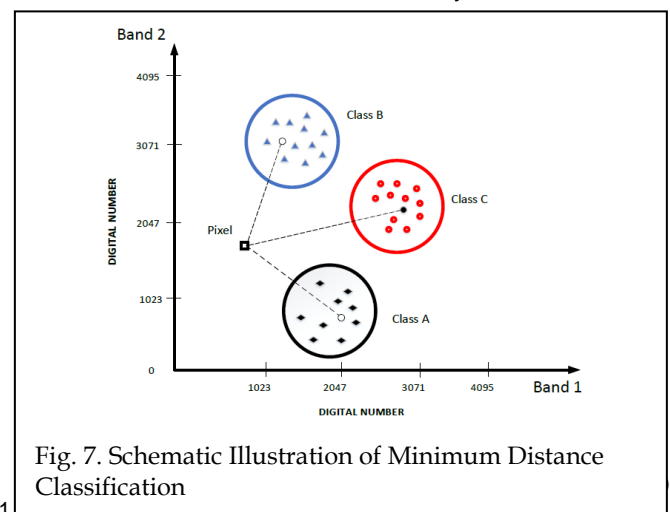
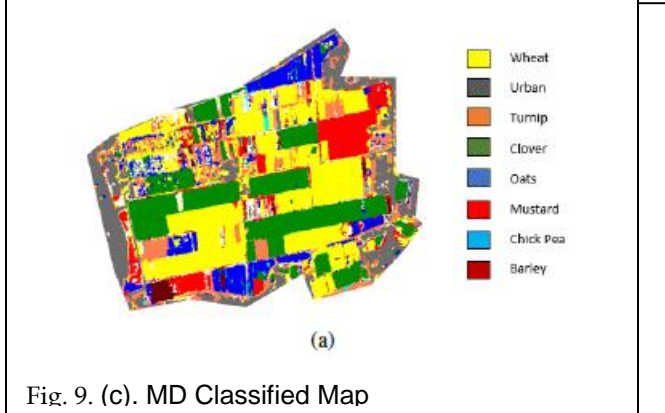
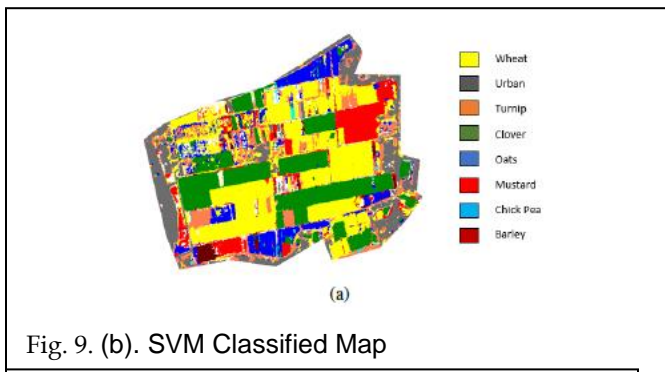
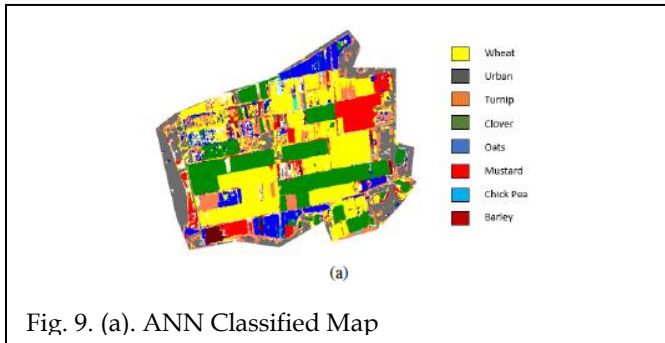


Fig. 7. Schematic Illustration of Minimum Distance Classification

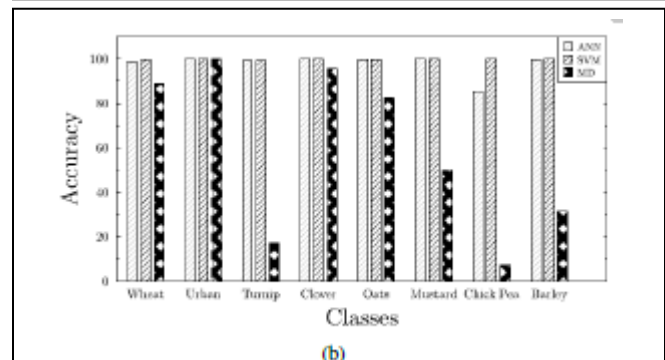
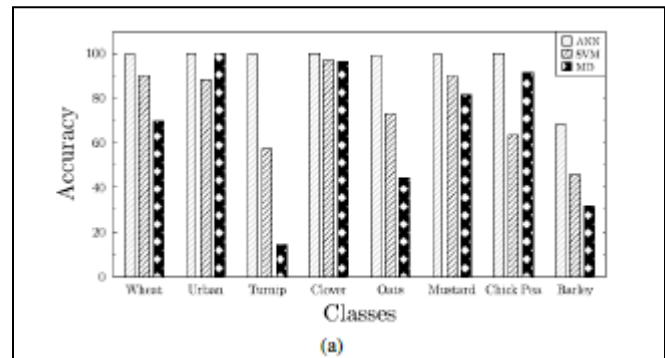
## 6 RESULTS AND DISCUSSION

Classification performance of the three different supervised classifiers i.e., ANN, SVM and MD is presented in the form of confusion matrix in Table 4, Table 5 and Table 6, respectively. The results have been calculated and assessed in terms of producer's accuracy, user's accuracy, overall accuracy and Kappa Coefficient. The classified map for all the three classifiers i.e., ANN, SVM and MD are shown in Figure 9(a), Figure 9(b) and Figure 9(c), respectively.



The Figure 8(a) shows the performance comparison between these three classifiers in terms of producer accuracy. It can be observed that the ANN classifier has better producer accuracy for the entire classes as compared to SVM and MD classifiers. More specifically, the producer accuracy for wheat class is 99:53% for ANN classifier, while SVM and MD classify with an accuracy of 90:30% and 69:58%, respectively. Thus, the ANN classifier has achieved better accuracy on the classification map with the least number of omission errors as compared to SVM and MD. Similarly, it can be observed that the user accuracy of the ANN classifier is higher than the other two techniques for most of the classes as clear from figure 8(b). However, it is observed that the ANN classifier has slightly

lower user accuracy for wheat, Oats and Chick Pea as compared to SVM classifier as clear from Figure 8(b). More specifically, the user accuracy of 98:95% for wheat class in ANN classifier is slightly lower than 99:56% user accuracy for SVM classifier, while MD has the lowest i.e. 89:01% user accuracy value. Therefore, it can be concluded that the SVM classifier has a marginal gain of 0:61% with reference to the user accuracy performance of the ANN classifier. However, keeping in view the performance gain of 9:23% in the producer accuracy of the ANN classifier with reference to the SVM classifier the marginal gain of 0:61% in the user accuracy of the SVM classifier has lower impact on the overall accuracy, relative to the ANN classifier. Furthermore, it is observed that although the user accuracy performance of both the ANN and SVM classifiers is better, the MD classifier has the lowest user accuracy performance for all the considered classes. The overall accuracy and Kappa Coefficient performance for all the three classifiers is presented in Figure 8(c). It is evident that the ANN classifier outperforms SVM and MD classifiers as shown in figure 8(c). The overall accuracy for ANN classifier is 98:7031% with a Kappa Coefficient of 0:9825, which is much higher than the SVM's overall accuracy of 85:2% and Kappa Coefficient of 0:81. Moreover, the MD classifier has the lowest overall accuracy of 73:1604% and Kappa Coefficient value of 0:646.



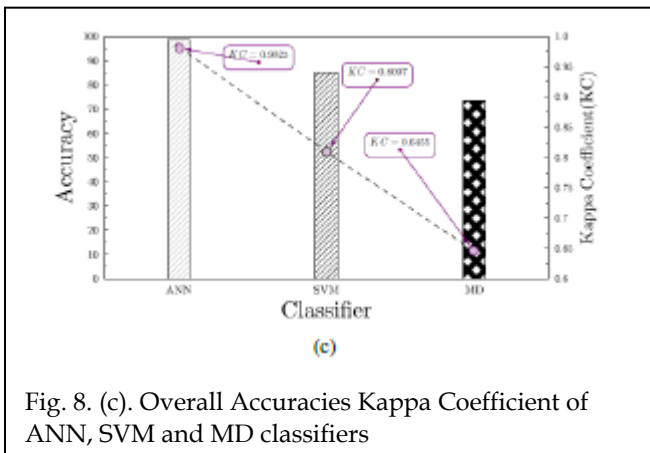


Fig. 8. (c). Overall Accuracies Kappa Coefficient of ANN, SVM and MD classifiers

## 7 CONCLUSION

Accurate and timely generation of agricultural crop statistics play a vital role in proper agricultural management. In this research paper, we focus on the land cover classification of wheat crop using remotely sensed multi-spectral planet-scope temporal data. Furthermore, we have utilized machine learning paradigm for the automated classification of land cover. The planet-scope imagery used in our research work is a temporal stack of multi-date imagery obtained on multiple dates with reference to the phenological wheat cycle. Furthermore, three different machine learning classifiers i.e. Artificial Neural Network (ANN), Support Vector Machine (SVM) and Minimum Distance (MD) classifiers are used for the wheat crop classification. Performance analysis of these classifiers is carried out with the aid of confusion matrix and Kappa Coefficient values. The results obtained show that the ANN classifier results in the best producer accuracy performance of 99:53% for the wheat class, while in SVM and MD it is 90:30% and 69:58%, respectively. Thus the ANN classifier results in better wheat classification accuracy in terms of classification of wheat on the classification map with the least number of omission errors as compared to both the SVM and MD classifiers. Furthermore, the ANN classifier with an overall accuracy of 98:70% and Kappa Coefficient value of 0:98 outperforms SVM and MD classifiers having an overall accuracy of 85.2005% and 73.1604% and Kappa Coefficient values of 0.8097 and 0.6455, respectively. Moreover, it is observed that the MD classifier has the lowest overall accuracy of 73:16% and Kappa Coefficient value of 0:64. In nutshell, the advanced machine learning techniques perform much better than the naive technique.

## ACKNOWLEDGMENTS

- The financial support of National Center of Big data and Cloud Computer (NCBC), University of Engineering and Technology, Peshawar, under the auspices of Higher Education Commission, Pakistan is gratefully acknowledged.
- The data-grant support of Planet INC in provisioning of Planet-Scope Dove Satellites Imagery is also gratefully acknowledged.

## REFERENCES

- [1] A. A. Chandio, J. Yuansheng, T. Rahman, M. N. Khan, X. Guangshun, and Z. Zhi, "Analysis of agricultural subsectors contribution growth rate in the agriculture gdp growth rate of pakistan," *International Journal of Humanities and Social Science Invention*, vol. 4, no. 8, pp. 101–105, 2015.
- [2] "Pakistan grain and feed annual," [://www.agripunjab.gov.pk/overview](http://www.agripunjab.gov.pk/overview)
- [3] "Agriculture department pakistan statistics," [https://apps.fas.usda.gov/newgainapi/api/report/downloadreportbyfilename?filename=Grain%20and%20Feed%20Annual\\_Islamabad\\_Pakistan\\_3-28-2019.pdf](https://apps.fas.usda.gov/newgainapi/api/report/downloadreportbyfilename?filename=Grain%20and%20Feed%20Annual_Islamabad_Pakistan_3-28-2019.pdf), accessed: 2020-05-2.
- [4] D. Poli, F. Remondino, E. Angiuli, and G. Agugiaro, "Radiometric and geometric evaluation of geoeye-1, worldview-2 and pléiades-1a stereoimages for 3d information extraction," *ISPRS Journal of Photogrammetry and Remote Sensing*, vol. 100, pp. 35–47, 2015.
- [5] R. Hooda, M. Yadav, and M. Kalubarme, "Wheat production estimation using remote sensing data: An indian experience," in *Workshop Proceedings: Remote Sensing Support to Crop Yield Forecast and Area Estimates*, Stresa, Italy. 30 Nov.–1 Dec. 2006., 2006, pp. 85–89.
- [6] M.-C. Cheng and C. Zhang, "Formosat-2 for international societal benefits," *Remote Sensing*, vol. 2016, 2016.
- [7] P. Team, "Planet application program interface: In space for life on earth," San Francisco, CA, vol. 2017, p. 40, 2017.
- [8] "Finance division," <http://www.finance.gov.pk>, accessed: 2020-02-2.
- [9] H. Mu, L. Zhou, X. Dang, and B. Yuan, "Winter wheat yield estimation from multitemporal remote sensing images based on convolutional neural networks," in *2019 10th International Workshop on the Analysis of Multitemporal Remote Sensing Images (MultiTemp)*. IEEE, 2019, pp. 1–4.
- [10] Ö. Vanlı, A. Sabuncu, and Z. D. U. Avci, "Regional classification of winter wheat using remote sensing data in southeastern turkey," in *2019 8th International Conference on Agro-Geoinformatics (Agro-Geoinformatics)*. IEEE, 2019, pp. 1–4.
- [11] F. Xu, Z. Li, S. Zhang, N. Huang, Z. Quan, W. Zhang, X. Liu, X. Jiang, J. Pan, and A. V. Prishchepov, "Mapping winter wheat with combinations of temporally aggregated sentinel-2 and landsat-8 data in shandong province, china," *Remote Sensing*, vol. 12, no. 12, p. 2065, 2020.
- [12] C.-j. Li, J.-h. Wang, W. Qian, D.-c. Wang, X.-y. Song, W. Yan, and W.-j. Huang, "Estimating wheat grain protein content using multitemporal remote sensing data based on partial least squares regression," *Journal of Integrative Agriculture*, vol. 11, no. 9, pp. 1445–1452, 2012.
- [13] P. Yang, Q. Zhou, Z. Chen, Y. Zha, W. Wu, and R. Shibasaki, "Estimation of regional crop yield by assimilating multi-temporal tm images into crop growth model," in *2006 IEEE International Symposium on Geoscience and Remote Sensing*. IEEE, 2006, pp. 2259–2262.
- [14] S. Xiaoyu, C. Bei, Y. Guijun, and F. Haikuan, "Comparison of winter wheat growth with multi-temporal remote sensing imagery," in *Proceedings of Conference Series on Earth and Environmental Science*, 2014, pp. 1–7.
- [15] J. Liu, P. Chen, and X. Xu, "Estimating wheat coverage using multispectral images collected by unmanned aerial vehicles and a new sensor," in *2018 7th International Conference on Agro-geoinformatics (Agrogeoinformatics)*. IEEE, 2018, pp. 1–5.
- [16] M. Du and N. Noguchi, "Monitoring of wheat growth status and mapping of wheat yield's within-field spatial variations using color images acquired from uav-camera system," *Remote sensing*, vol. 9, no. 3, p. 289, 2017.
- [17] W. Zhuo, J. Huang, L. Li, X. Zhang, H. Ma, X. Gao, H. Huang, B. Xu, and X. Xiao, "Assimilating soil moisture retrieved from sentinel-1 and sentinel-2 data into wofost model to improve winter wheat yield estimation," *Remote Sensing*, vol. 11, no. 13,

- p. 1618, 2019.
- [18] L. Liangyun, W. Jihua, S. Xiaoyu, L. Cunjun, H. Wenjiang, and Z. Chunjiang, "Study on winter wheat yield estimation model based on ndvi and seedtime," in IGARSS 2004. 2004 IEEE International Geoscience and Remote Sensing Symposium, vol. 6. IEEE, 2004, pp. 4045–4047.
- [19] N.-B. Chang, C. Mostafiz, Z. Sun, W. Gao, and C.-F. Chen, "Developing a prototype satellite-based cyber-physical system for smart wastewater treatment," in 2017 IEEE 14th International Conference on Networking, Sensing and Control (ICNSC). IEEE, 2017, pp. 339–344.
- [20] Y. Zhongcheng, W. Fengge, and Z. Junsuo, "Research of a construction method of space-based cyber-physical system," in 2016 Chinese Control and Decision Conference (CCDC). IEEE, 2016, pp. 6862–6866.
- [21] A. Mirkouei, "A cyber-physical analyzer system for precision agriculture," *J Environ Sci Curr Res*, vol. 3, p. 016, 2020.
- [22] National Center for Big Data Cloud Computing, UET Peshawar, GeoSurvey. [Online]. Available: <https://play.google.com/store/apps/details?id=com.ncbc.survey.gis&hl=en>
- [23] K. Perumal and R. Bhaskaran, "Supervised classification performance of multispectral images," *arXiv preprint arXiv:1002.4046*, 2010.
- [24] M. A. Hearst, S. T. Dumais, E. Osuna, J. Platt, and B. Scholkopf, "Support vector machines," *IEEE Intelligent Systems and their applications*, vol. 13, no. 4, pp. 18–28, 1998.
- [25] M. Ustuner, F. B. Sanli, and B. Dixon, "Application of support vector machines for land use classification using high-resolution rapid eye images: A sensitivity analysis," *European Journal of Remote Sensing*, vol. 48, no. 1, pp. 403–422, 2015.
- [26] A. Wacker and D. Landgrebe, "Minimum distance classification in remote sensing," *LARS Technical Reports*, p. 25, 1972.
- [27] K. Yang, A. Pan, Y. Yang, S. Zhang, S. H. Ong, and H. Tang, "Remote sensing image registration using multiple image features," *Remote Sensing*, vol. 9, no. 6, p. 581, 2017.
- [28] B. Ankayarkanni and A. E. S. Leni, "A new statistical rule model for image retrieval system of remote sensing images," in 2016 International Conference on Circuit, Power and Computing Technologies (ICCPCT). IEEE, 2016, pp. 1–5